

# Pan-cancer analysis reveals nucleolar and spindle-associated protein 1 as a predictive marker for human cancer

## **Jiehua Zheng**

Department of General Surgery, The Second Affiliated Hospital of Shantou University Medical College, Shantou, Guangdong, China

## **Yaokun Chen**

Department of General Surgery, The Second Affiliated Hospital of Shantou University Medical College, Shantou, Guangdong, China

## **Jinyao Wu**

Department of General Surgery, The Second Affiliated Hospital of Shantou University Medical College, Shantou, Guangdong, China

## **Daitian Zheng**

Department of General Surgery, The Second Affiliated Hospital of Shantou University Medical College, Shantou, Guangdong, China

## **Yiyuan Liu**

Department of General Surgery, The Second Affiliated Hospital of Shantou University Medical College, Shantou, Guangdong, China

## **Jiehui Cai**

Department of General Surgery, The Second Affiliated Hospital of Shantou University Medical College, Shantou, Guangdong, China

## **Lingzhi Chen**

Department of General Surgery, The Second Affiliated Hospital of Shantou University Medical College, Shantou, Guangdong, China

## **Zeqi Ji**

Department of General Surgery, The Second Affiliated Hospital of Shantou University Medical College, Shantou, Guangdong, China

## **Huiting Tian**

Department of General Surgery, The Second Affiliated Hospital of Shantou University Medical College, Shantou, Guangdong, China

## **Qiuping Yang**

Department of General Surgery, The Second Affiliated Hospital of Shantou University Medical College, Shantou, Guangdong, China

## **Yexi Chen**

Department of General Surgery, The Second Affiliated Hospital of Shantou University Medical College, Shantou, Guangdong, China

**Zhiyang Li** (✉ [s\\_zyli4@stu.edu.cn](mailto:s_zyli4@stu.edu.cn))

Department of General Surgery, The Second Affiliated Hospital of Shantou University Medical College, Shantou, Guangdong, China

---

## Research Article

**Keywords:** NUSAP1, pan-cancer analysis, prognosis, phosphorylation, survival analysis

**Posted Date:** June 22nd, 2022

**DOI:** <https://doi.org/10.21203/rs.3.rs-1761668/v1>

**License:**   This work is licensed under a Creative Commons Attribution 4.0 International License.

[Read Full License](#)

---

# Abstract

Understanding the driving factors and the common and unique mechanisms of human tumorigenesis is essential for the development of effective treatments. As a potential oncogene, nucleolar and spindle-associated protein 1 (*NUSAP1*) participates in the regulation of a variety of tumor cells (e.g. hepatocellular carcinoma), lung cancer proliferation, metastasis, and drug resistance. However, a systematic pan-cancer analysis has not yet been carried out. Using The Cancer Genome Atlas and Gene Expression Omnibus datasets, the Human Protein Atlas, and several bioinformatics tools, we investigated the expression and potential carcinogenic effects of *NUSAP1* in 33 tumors. We found that *NUSAP1* overexpression usually indicated poor overall survival in patients with tumors with high *NUSAP1* expression, such as lung cancer, breast cancer, and hepatocellular carcinoma. We also analyzed the *NUSAP1* mutation burden in cancers and *NUSAP1*-related survival in patients with tumors, compared *NUSAP1* phosphorylation in normal and primary tumor tissues, and explored possible functional mechanisms of *NUSAP1*-mediated tumorigenesis. The current pan-cancer analysis provides a relatively comprehensive overview of the carcinogenic effects of *NUSAP1* in a variety of human cancers, which may stimulate new ideas for treating several tumors.

## 1 Introduction

Cancer is a major public health problem worldwide. Given the complexity of tumors, conducting a pan-cancer expression analysis of genes, and assessing their relevance to the clinical prognosis and the potential molecular mechanisms is very important. A large number of tumor-related functional genomics datasets are available for multiple cancers, allowing a detailed downstream pan-cancer analysis, including publicly funded cancer genomics databases and repositories such as The Cancer Genome Atlas (TCGA) and Gene Expression Omnibus (GEO) (Blum et al. 2018, Tomczak et al. 2015, Clough and Barrett 2016).

Nucleolar and spindle-associated protein 1 (*NUSAP1*) is a microtubule-binding protein that plays an important role in mitosis, spindle assembly, and stability (Li et al. 2016, Ribbeck et al. 2006). Two direct effects of *NUSAP1* on microtubules have been revealed in *in vitro* reconstitution experiments. On one hand, *NUSAP1* can efficiently stabilize microtubules against depolymerization. On the other hand, it can cross-link a large number of microtubules into aster-like structures, thick fibers, and networks [5]. *NUSAP1* is highly expressed in various cancers, such as metastatic prostate cancer (Kokkinakis et al. 2005, Ryu et al. 2007, Gordon et al. 2017, Chen et al. 2010, Liu et al. 2015, Cuzick et al. 2011, Li et al. 2019, Roy et al. 2018). In addition, high *NUSAP1* expression is known to be related to a poor clinical prognosis for several types of tumors, including prostate cancer, cervical cancer, estrogen receptor-positive breast cancer, and hepatocellular carcinoma (Liu et al. 2015, Cuzick et al. 2011, Li et al. 2019, Roy et al. 2018). However, previous studies have limited the evaluation of *NUSAP1* to a few cancer types; accordingly, its role in other tumor types remains elusive. Therefore, we used TCGA and GEO databases to explore *NUSAP1* expression profiles across various tumor types in a pan-cancer analysis. We also considered other aspects, such as survival status, genetic alterations, protein phosphorylation, etc. This comprehensive

analysis aimed to reveal the underlying molecular mechanisms of NUSAP1 in the pathogenesis and clinical prognosis in a variety of human cancers.

## 2 Materials And Methods

### 2.1 Gene expression analysis

We input “NUSAP1” in the “Gene\_DE” module in the Tumor Immune Estimation Resource, version 2 (TIMER2; <http://timer.cistrome.org/>) to evaluate differences in NUSAP1 expression between tumor and adjacent normal tissues for various tumors and specific tumor subtypes included in the TCGA database. For tumors without, or with only limited, normal tissue data (e.g., acute myeloid leukemia [LAML], thymoma [THYM], etc.), we used the Gene Expression Profiling Interactive Analysis, version 2 (GEPIA2; <http://gepia2.cancer-pku.cn/#analysis>) (Tang et al. 2019) to acquire box plots of Genotype-Tissue Expression (GTEx) data, under the following settings: P-value cutoff, 0.01; log<sub>2</sub>-fold change cutoff, 1; and “Match TCGA normal and GTEx data.” In addition, via the “Pathological Staging Diagram” module in GEPIA2, we obtained violin plots of NUSAP1 expression in all TCGA tumors in different pathological stages (stages I, II, III, and IV). Transformed expression data (log<sub>2</sub> transcripts per million [TPM] + 1) were submitted to the box and violin plots.

The UALCAN portal (<http://ualcan.path.uab.edu/analysis-prot.html>) is an interactive web resource for analyzing cancer-omics data, allowing a protein expression analysis of the Clinical Proteomic Tumor Analysis Consortium (CPTAC) dataset (Chen et al. 2019). We analyzed and compared the total protein and phosphoprotein expression levels of NUSAP1 between primary and normal tissues, including breast cancer, liver cancer, ovarian cancer, and lung carcinoma.

### 2.2 Immunohistochemistry (IHC) staining

The Human Protein Atlas (HPA; <http://www.proteinatlas.org/>) was used to compare and analyze NUSAP1 expression differences between normal tissues and three tumor tissues, including liver hepatocellular carcinoma (LIHC), lung adenocarcinoma (LUAD), and ovarian serous cystadenocarcinoma (OV).

### 2.3 Survival prognosis analysis

To acquire overall survival (OS) and disease-free survival (DFS) significance map data for NUSAP1, across all TCGA tumors, we used the Kaplan-Meier “Survival Map” module of GEPIA2 (Chen et al. 2019). As expression thresholds, cutoff-high (50%) and cutoff-low (50%) values were used to split the dataset into high-expression and low-expression cohorts. For hypothesis testing, we adopted the log-rank test, and survival plots were also obtained using the Kaplan-Meier “Survival Analysis” module of GEPIA2.

### 2.4 Genetic alteration analysis

The cBioPortal tool (<https://www.cbioportal.org/>) was used to conduct a genetic alteration analysis. In order to investigate the genetic alteration characteristics of NUSAP1, we selected “TCGA Pan Cancer Atlas

Studies" in the "Quick select" section, and entered "NUSAP1", which collected data on the alteration frequency, mutation types, mutation sites, and copy number alterations (CAN) in the protein structure for all TCGA tumors. Using the three-dimensional (3D) structure of NUSAP1, indicated by the "Mutations" module, we obtained mutation site information for NUSAP1. In addition, to collect data on differences in the OS, DFS, and progression-free survival (PFS) between TCGA cancer cases with and without NUSAP1 genetic alterations, the "Comparison" module was applied, creating Kaplan-Meier plots with log-rank P-values.

## 2.5 Immune infiltration analysis

We used the "Immune-Gene" module of TIMER2 to analyze the relationship between NUSAP1 expression and immune infiltrates across all TCGA tumors. B cells, cluster of differentiation 8-positive (CD8+) T cells, CD4+ T cells, macrophages, neutrophils, and dendritic cells (DCs) were selected for detailed analysis. Across 39 TCGA cancer types, we analyzed the correlation between NUSAP1 expression and tumor infiltration for four immunosuppressive cell types known to promote T-cell rejection; namely, myeloid-derived suppressor cells (MDSCs), cancer-associated fibroblasts (CAFs), and M2 subtype of tumor-associated macrophages (M2-TAMs), and regulatory T cells (Tregs). The correlation was described by the purity-adjusted partial Spearman's rho value and statistical significance ( $P < 0.05$ ). GraphPad Prism software (ver. 8.0.0 for Windows) was used for data visualization. Heatmaps were used to observe the level of immune cell infiltration in 33 TCGA cancers. For the evaluation of the influence of NUSAP1 genetic and epigenetic changes on the phenotype of dysfunctional T cells, the "Query Gene" module, with the tumor immune dysfunction and exclusion (TIDE) algorithm, was considered as a reliable method.

## 2.6 NUSAP1-related gene enrichment analysis

We searched the STRING website (<https://string-db.org/>) using a single protein name ("NUSAP1") and organism ("Homo sapiens") in the query. We then set the following main parameters: minimum required interaction score, "Low confidence [0.150]"; meaning of network edges, "evidence"; maximum number of interactors to be displayed, "no more than 50 interactors" in the 1st shell; and active interaction sources, "experiments". We obtained experimentally determined NUSAP1-binding proteins using this method. Based on TCGA tumor and normal tissue datasets, we used the "Similar Gene Detection" module in GEPIA2 to obtain the top 100 NUSAP1-correlated genes. We also conducted a pairwise gene-gene Pearson correlation analysis of *NUSAP1* and selected genes. Log<sub>2</sub> [TPM + 1] data was used for the dot plot. The *P*-values and correlation coefficients (R) were also calculated.

The heatmap of the selected gene expression profiles represents the partial correlation and P value in the Spearman rank correlation test, with purity adjustment. As an interactive Venn diagram viewer, Jvenn (Bardou et al. 2014) was applied in an intersection analysis comparing the genes that NUSAP1 binds to and interacts with. Furthermore, we combined these two datasets to conduct a Kyoto Encyclopedia of Genes and Genomes (KEGG) pathway analysis. Finally, the "tidyr" and "ggplot2" R packages were used to reveal enriched pathways. Furthermore, we conducted a gene ontology (GO) enrichment analysis using the "clusterProfiler" R software package. Using the cnetlot function (Circle = F, ColorEdge = T, Node\_Label

= T), biological process, cell component, and molecular function data were visualized as netlots. R language software (R-3.6.3, 64-bit) (<https://www.r-project.org/>) was used for analysis and the statistical significance was set at  $P < 0.05$ .

## 3 Results

### 3.1 Gene expression analysis data

In this study, we aimed to conduct a comprehensive analysis of the oncogenic role of human NUSAP1 (mRNA, NM\_001243144.2; protein, NP\_001230073.1; Figure S1). We analyzed NUSAP1 expression patterns in various cell lines and non-tumor tissues. Additionally, we acquired data from HPA, GTEx, and Function Annotation of the Mammalian Genome 5 (FANTOM5) datasets, which are shown in Figure S2A. Based on this analysis, NUSAP1 has its highest expression in the thymus, followed by bone marrow and the appendix, and its mRNA tissue specificity showed group enrichment (bone marrow and lymphoid tissue). HPA/Monaco/Schmiedel datasets were used to analyze NUSAP1 expression in different blood cells, and Treg cell RNA specificity was enhanced (Figure S2B).

We then applied the TIMER2 method to compare NUSAP1 expression levels between tumor and adjacent normal tissues in the TCGA dataset. As shown in Fig. 1A, NUSAP1 expression levels in the tumor tissues of bladder urothelial carcinoma (BLCA), breast invasive carcinoma (BRCA), cholangiocarcinoma (CHOL), colon adenocarcinoma (COAD), esophageal carcinoma (ESCA), head and neck squamous cell carcinoma (HNSC), kidney renal clear cell carcinoma (KIRC), kidney renal papillary cell carcinoma (KIRP), LIHC, LUAD, lung squamous cell carcinoma (LUSC), prostate adenocarcinoma (PRAD), rectum adenocarcinoma (READ), stomach adenocarcinoma (STAD), thyroid carcinoma (THCA), and uterine corpus endometrial carcinoma (UCEC) were higher than those in the corresponding control tissues. Only kidney chromophobe (KICH) did not show differential expression.

Using the GTEx dataset for tumors lacking normal tissue data, we further evaluated NUSAP1 expression differences between tumor and normal tissues. We found significant differences between tumor and normal tissues for cervical squamous cell carcinoma and endocervical adenocarcinoma (CESC), lymphoid neoplasm diffuse large B-cell lymphoma (DLBC), glioblastoma multiforme (GBM), brain lower grade glioma (LGG), OV, pancreatic adenocarcinoma (PAAD), sarcoma (SARC), skin cutaneous melanoma (SKCM), testicular germ cell tumors (TGCT), THYM, and uterine carcinosarcoma (UCS) (Fig. 1B,  $P < 0.05$ ). In contrast, we found no significant differences for adrenocortical carcinoma (ACC), LAML, and pheochromocytoma and paraganglioma (PCGC) (Figure S3). Overall, we found that NUSAP1 expression is elevated in most human tumors.

In addition, using the CPTAC dataset, we evaluated NUSAP1 at the protein level. The expression level of NUSAP1 total protein in breast cancer, clear cell renal cell carcinoma (RCC), colon cancer, LUAD, ovarian cancer, and UCEC tissues was higher than that in normal tissues (Fig. 2A,  $P < 0.001$ ).

The “Pathological Stage Plot” module of HEPIA2 tool was used to analyze the relationship between NUSAP1 expression and tumor pathological staging. We found that NUSAP1 expression underwent stage-specific changes in some tumor types, including ACC, BRCA, KICH, KIRC, KIRP, LIHC, LUAD, SKCM, and THCA (Fig. 2B, all  $P < 0.05$ ), but not in other tumor types (Figure S4).

Moreover, the IHC results, provided by the HPA database, were compared to TCGA NUSAP1 gene expression data. The data analysis results for the two databases were consistent. NUSAP1 IHC staining in normal liver, lung, and ovary tissues was negative or medium, while medium or strong staining was observed in corresponding tumor tissues (Figs. 3A–C).

### 3.2 Survival analysis data

We aimed to understand the relationship between NUSAP1 expression, prognosis, and OS. Based on the NUSAP1 expression level, tumor cases were divided into high-expression and low-expression groups, and the correlation between NUSAP1 expression and prognosis in patients with different tumors was determined, mainly using the TCGA and GEO datasets. High NUSAP1 expression was related to a poor OS prognosis for ACC ( $P = 0.038$ ), KIRP ( $P = 0.00012$ ), LGG ( $P = 3.6e-07$ ), LIHC ( $P = 0.0063$ ), LUAD ( $P = 0.00051$ ), mesothelioma(MESO) ( $P = 7e-05$ ), PAAD ( $P = 0.0046$ ), and PRAD ( $P = 0.02$ ) (Fig. 4A). High NUSAP1 expression was related to a poor DFS prognosis for ACC ( $P = 5e-04$ ), KIRP ( $P = 0.00016$ ), LGG ( $P = 1.3e-05$ ), LIHC ( $P = 7e-04$ ), LUAD ( $P = 0.017$ ), PAAD ( $P = 0.0049$ ), PRAD ( $P = 0.0018$ ), SARC ( $P = 0.03$ ), and uveal melanoma (UVM) ( $P = 0.00035$ ) (Fig. 4B). Additionally, low NUSAP1 expression was related to a poor OS prognosis for THYM ( $P = 0.0049$ ) (Fig. 4A).

Next, we analyzed the survival data using the Kaplan-Meier plotter tool and noted a relationship between high NUSAP1 expression and poor OS and post-progression survival (PPS) for gastric cancer; poor OS, first progression (FP) and PPS for lung cancer; poor OS for ovarian cancer; poor OS, relapse-free survival (RFS), distant metastasis-free survival (DMFS), and PPS for breast and liver cancers (Figure S5). In contrast, we failed to detect the correlation between expression of NUSAP1 and the prognosis of gastric cancer FP, ovarian cancer FP and PPS.

### 3.3 Genetic alteration analysis data

We explored NUSAP1 genetic alterations in human tumor samples. With “mutation” as the main type, the highest alteration frequency of NUSAP1 ( $> 3\%$ ) occurred in patients with uterine tumors. In the “amplification” type of CNA, sarcoma had the highest alteration frequency (approximately 1%). All cases of mesothelioma, DLBC, UCS, and esophageal adenocarcinoma had NUSAP1 copy number deletions, with genetic alteration frequencies of more than 4% for the first two tumors (Fig. 5A). Figure 5B shows the types, locations, and numbers of NUSAP1 genetic alterations. We did not find major types of genetic alterations, and the missense mutation, R249\*/Q alteration, was exclusively detected in two cases of UCEC. In addition, we observed the R249 site in the 3D structure of NUSAP1 (Fig. 5C). Furthermore, we systematically evaluated the potential link between NUSAP1 genetic alterations and the clinical survival prognosis of patients with various types of cancer. Figure 5D shows that the PFS prognosis ( $P = 0.0306$ )

in patients with UCEC with a *NUSAP1* alteration was better, but the OS ( $P = 0.0850$ ), PFS ( $P = 0.118$ ), and disease-specific survival ( $P = 0.228$ ) were not significantly different, than that in patients with no *NUSAP1* alterations (Fig. 5D).

We went a step further to probe the correlation between *NUSAP1* expression and the tumor mutational burden (TMB) and microsatellite instability (MSI) for all tumors in the TCGA. We found a positive correlation between *NUSAP1* expression and TMB for BLCA ( $P = 1.9e-06$ ), BRCA ( $P = 2.3e-019$ ), COAD ( $P = 6e-06$ ), KICH ( $P = 0.0038$ ), KIRC ( $P = 0.025$ ), LGG ( $P = 1.5e-17$ ), LUAD ( $P = 3.3e-19$ ), PAAD ( $P = 7e-08$ ), PRAD ( $P = 6.2e-17$ ), SARC ( $P = 0.00021$ ), SKCM ( $P = 1.3e-05$ ), COAD ( $P = 1.6e-23$ ), and UCEC ( $P = 2.1e-06$ ), and a negative correlation for ESCA ( $P = 0.025$ ) and THYM ( $P = 2.5e-12$ ) (Figure S6). In addition, *NUSAP1* expression was positively correlated with MSI for CHOL ( $P = 0.0076$ ), COAD ( $P = 1.2e-07$ ), LUSC ( $P = 0.0013$ ), READ ( $P = 2e-04$ ), SARC ( $P = 0.00019$ ), STAD ( $P = 5.5e-08$ ), and UCEC ( $P = 2.1e-13$ ), and was negatively correlated with MSI for DLBC ( $P = 0.00014$ ) (Figure S7). In summary, these findings indicate that *NUSAP1* genetic alterations may be viewed as possible drivers of the tumors mentioned above.

### 3.4 Protein phosphorylation analysis data

The phosphorylation-dephosphorylation cascade plays a key role in tumorigenesis. We compared the *NUSAP1* phosphorylation levels between normal and primary tumor tissues. The CPTAC database, which includes breast and ovarian cancers, was used to analyze two types of tumors in detail. The *NUSAP1* phosphorylation sites were at S134, T181, and T312, which showed significant differences in ovarian, but not breast, cancer (Fig. 6A). The *NUSAP1* phosphorylation level at the T181 locus in breast cancer tissues was not different from that in normal tissues (Fig. 6B). The phosphorylation level was significantly increased in ovarian cancer at the T181 and T312 loci, while it was reduced at the S134 locus (Fig. 6C).

### Immune infiltration analysis data

It is well known that tumor-infiltrating immune cells, an important part of the tumor microenvironment, are closely associated with cancer occurrence, development, and metastasis (Fridman et al. 2011, Steven and Seliger 2108). In tumor microenvironmental stroma, tumor-associated fibroblasts are involved in regulating the functions of all kinds of tumor-infiltrating immune cells (Chen and Song 2019, Kwa et al. 2019). *NUSAP1* overexpression causes the bundling of cytoplasmic microtubules (Raemaekers et al. 2003); therefore, we predicted that the *NUSAP1* expression level or genetic changes in *NUSAP1* may affect the response of tumor-infiltrating immune cells. Based on this, we explored the correlation between the level of infiltration of various immune cells and *NUSAP1* expression in a variety of tumor types in the TCGA dataset. It should be noted that *NUSAP1* expression was positively correlated with the estimated infiltration value of six immune cell types (B cells, CD8 + T cells, CD4 + T cells, macrophages, neutrophils, and DCs) for HNSC, LGG, and LIHC (Fig. 7A). Figure 7B shows the correlation between the *NUSAP1* expression level and the infiltration of four immunosuppressive cells (CAFs, M2-TAMs, MDSCs, and Treg cells) that are known to promote T-cell exclusion. *NUSAP1* expression was positively correlated with

MSDC tumor infiltration in almost all tumors (except CESC, DLBC, HNSC-human papilloma virus-positive, TGCT, and THCA), Treg tumor infiltration in PRAD, and CAF tumor infiltration in BRCA, TGCT, and THYM. However, NUSAP1 expression was not correlated with M2-TAM tumor infiltration in any cancer. We assessed the relevance of NUSAP1 biomarkers by comparing the response results of NUSAP1 and standardized biomarkers to immune checkpoint blocking (ICB) subgroups, as well as the predictive power for OS. Custom exhibited a higher predictive value than TMB, T. Clonality, and B. Clonality, which had areas under the curve (AUCs) > 0.5 in eight, nine, and seven ICB sub-cohorts, respectively. Additionally, the predictive power was comparable to that of Merck 18, but lower than that of TIDE, MSI.Score, CD274, CD8, and interferon- $\gamma$ (IFNG) (Fig. 8A). Furthermore, we evaluated the influence of genetic and epigenetic changes in NUSAP1 on the phenotype of dysfunctional T cells. The results showed high NUSAP1 expression as related to a poor prognosis for programmed death 1 protein (PD1) in melanoma (ICB\_Gide2019\_PD1 + CTLA4), adoptive cell transfer (ACT) in melanoma (ICB\_Lauss2017\_ACT), and PD1 in melanoma (ICB\_Riaz2017\_PD1). Additionally, in an analysis of gene knockout phenotypes, we noted that NUSAP1-knockout had a significant impact on lymphocyte-mediated tumor killing in Mel624 melanoma (Patel 2017 1) and T-cell (Shifrut 2018 Average) models (Fig. 8B).

### 3.5 Enrichment analysis of NUSAP1-related partners

Finally, we screened for NUSAP1 interacting proteins and NUSAP1 expression-related genes, and performed a series of pathway enrichment analyses to further investigate how the molecular mechanisms of *NUSAP1* are involved in tumorigenesis and development. By applying the STRING tool, we acquired data on 30 NUSAP1 binding proteins detected in experiments. The interaction network of these 30 proteins is shown in Fig. 9A. We also used the GEPIA2 tool to combine all tumor expression data from the TCGA dataset and obtain the top 100 genes related to NUSAP1 expression. NUSAP1 expression was positively correlated with that of cyclin F (CCNF;  $R = 0.73$ ), chromatin assembly factor 1 subunit A (CHAF1A;  $R = 0.71$ ), kinesin family member 14 (KIF14;  $R = 0.77$ ), kinesin family member 20A (KIF20A;  $R = 0.78$ ), and thymopoietin (TMPO;  $R = 0.78$ ) (Fig. 9B). The heatmap showed that in most cancer types, NUSAP1 was strongly and positively correlated with the above five genes (Fig. 9C). The intersection analysis of the above two sets of data also indicated the above five common members (Fig. 9D).

We integrated these two datasets for KEGG and GO enrichment analyses. The KEGG analysis showed that the role of NUSAP1 in tumor pathogenesis may be connected with the "Cell cycle" and "Mismatch repair" (Fig. 9E). Furthermore, the GO enrichment analysis data showed that NUSAP1 mostly acted on chromosomal regions, chromosomal segregation, and mitotic nuclear division (Fig. 9F).

## 4 Discussion

As a mitotic phosphorylation protein that binds to microtubules, NUSAP1, which can be selectively expressed in proliferating cells, is related to the stability of the spindle, and participates in the biological processes of chromosome separation and cell division (Ribbeck et al. 2006, Raemaekers et al. 2003, Ribbeck et al. 2007, Vanden Bosch et al. 2010, Xie et al. 2011, Chou et al. 2011, Mills et al. 2017).

NUSAP1 is highly conserved among higher eukaryotes, and is overexpressed in many malignant tumors (Chen et al. 2015). NUSAP1 was identified as a marker gene overexpressed in invasive cancer and was predicted to be a new tumor marker in 2011 (Nie et al. 2010). NUSAP1 has gradually become a focus in various tumor studies. However, whether NUSAP1 affects the pathogenesis of different tumors through common molecular mechanisms is still poorly understood. Therefore, based on combined data from the CPTAC, TCGA, and GEO databases, with data on the molecular characteristics of gene expression, gene changes, and protein phosphorylation, we performed a pan-cancer analysis of *NUSAP1* in 33 different tumors.

NUSAP1 was highly expressed in most tumors; however, its expression levels in ACC, LAML, and PCPG were lower than those in the corresponding control tissues. In addition, the current analysis showed that NUSAP1 overexpression in BRCA, LIHC, LUAD, and OV usually indicates a poor OS, which is consistent with the results of existing studies (Zhang et al. 2018, Roy et al. 2018, Ling et al. 2021, Zhang et al. 2020). For lung cancers, we evaluated LUSC (n = 501) and LUAD (n = 515) data from the TCGA dataset, and found that high NUSAP1 expression was related to a poor prognosis in terms of the OS ( $P = 0.00059$ ) and DFS ( $P = 0.017$ ) for LUAD, which may be associated with regulation of the BTG2/PI3K/Akt signaling pathway (Xu et al. 2020), but was not related to the prognosis in LUSC. Additionally, in PAAD, high NUSAP1 expression was associated with a poor prognosis. Furthermore, NUSAP1 affected the DFS in UVM. The mechanism of NUSAP1 in UVM is rarely reported; therefore, our analysis may indicate a new clinical biomarker for predicting the DFS in patients with UVM. Experiments show that NUSAP1 can significantly enhance the proliferation and colony-forming ability of OV cells. In addition, flow cytometry was confirmed that NUSAP1 knockdown promotes OV cell apoptosis and G2 phase arrest. Importantly, the Transwell experiment demonstrated that NUSAP1 silencing significantly inhibits the migration and invasion of OV cells. Overall, *NuSAP1* can significantly enhance the growth of OV cells, accelerate the cell cycle process, and enhance the migration and invasion capabilities of OV cells (Xu et al. 2020). However, in the TCGA-OV and TCGA-DFS cohorts, we failed to find a connection between NUSAP1 expression and the survival prognosis in patients with OV. It is worth noting that, based on the Kaplan-Meier plotter dataset containing GEO data, high NUSAP1 expression was associated with OS, but not with FP and PPS, in ovarian cancer. This result may be related to factors such as an insufficient number of cases and collected samples, which is worthy of further exploration.

Some studies have reported that high NUSAP1 expression is closely linked to breast cancer, and may be used as an early molecular marker of breast cancer (Kretschmer et al. 2011). NUSAP1 expression can promote invasive breast cancer cell proliferation, migration, and invasion by regulating the expression of cyclin D kinase (CDK1) and DLG-associated protein 5 (DLGAP5), and reduced susceptibility to epirubicin in invasive breast cancer cells, thereby affecting the efficacy of chemotherapy (Roy et al. 2018). Our study demonstrated that high NUSAP1 expression in breast cancer is positively correlated with poor OS, RFS, DMFS, and PPS prognosis. Therefore, it is necessary to further verify the mechanism of action of NUSAP1 in different types of breast cancer through experiments. We have presented evidence for a connection between NUSAP1 expression and MSI or TMB in all TCGA tumors. Furthermore, we conducted a series of enrichment analyses to determine the potential impact on the etiology and pathogenesis of

cancer by integrating information on NUSAP1 expression-related genes in all tumors. The T-cell rejection mechanism, viewed as a second mechanism of tumor immune escape (Joyce and Fearon 2015), can cause tumors to resist the infiltration of immune cells. T-cell rejection depends on the infiltration of immunosuppressive cells, such as CAFs, Tregs, M2-TAMs, and MDSCs; thus, infiltration is considered to be a biomarker of T-cell rejection in cancer (Komohara et al. 2016). In particular, the expression NUSAP1 level has a good correlation with the expression of immunosuppressive cells in almost all cancer types. Therefore, we speculate that T-cell rejection is one of the main mechanisms by which NUSAP1 regulates immune cells to escape tumors and promote tumor growth and metastasis.

In conclusion, this comprehensive pan-cancer analysis of NUSAP1, the first of its kind, demonstrated that there are statistical correlations between NUSAP1 expression and the clinical prognosis, protein phosphorylation, TMB, immune cell infiltration, and MSI across multiple tumor types. These results contribute to clarifying and comprehending the role of NUSAP1 in tumorigenesis from various perspectives. Based on the present analysis, we speculate that NUSAP1 may be used as a therapeutic target for many metastatic tumors, such as liver metastases in breast cancer and lung metastases in liver cancer, providing guidance for further investigations.

## Abbreviations

ACC, adrenocortical carcinoma; AUC, area under the curve; BLCA, bladder urothelial carcinoma; BRCA, breast invasive carcinoma; CAF, cancer-associated fibroblast; CCNF, cyclin F; CD cluster of differentiation; CDK1, cyclin D kinase; CESC, cervical squamous cell carcinoma and endocervical adenocarcinoma; CHAF1A, chromatin assembly factor 1 subunit A; CHOL, cholangiocarcinoma; CAN copy number alterations; COAD, colon adenocarcinoma; CPTAC, Clinical Proteomic Tumor Analysis Consortium; DC, dendritic cell; DFS, disease-free survival; DLBC, lymphoid neoplasm diffuse large B-cell lymphoma; DLGAP5, DLG-associated protein 5; DMFS, distant metastasis-free survival; ESCA, esophageal carcinoma; FANTOM5, Function Annotation of the Mammalian Genome 5; FPS, first progression survival; GBM, glioblastoma multiforme; GEO, Gene Expression Omnibus; GEPIA2, Gene Expression Profiling Interactive Analysis, version 2; GO, gene ontology; GTEx, Genotype-Tissue Expression; HNSC, head and neck squamous cell carcinoma; ICB, immune checkpoint blocking; IHC, immunohistochemistry; KEGG, Kyoto Encyclopedia of Genes and Genomes; KICH, kidney chromophobe; KIF14, kinesin family member 14; KIF20A, kinesin family member 20A; KIRC, kidney renal clear cell carcinoma; KIRP, kidney renal papillary cell carcinoma; LAML, acute myeloid leukemia; LGG, brain lower grade glioma; LIHC, hepatocellular carcinoma; LUAD, lung adenocarcinoma; LUSC, lung squamous cell carcinoma; M2-TAM, M2 subtype of tumor-associated macrophage; MDSC, myeloid-derived suppressor cell; MSI, microsatellite instability; NUSAP1, nucleolar and spindle-associated protein 1; OS, overall survival; OV, ovarian serous cystadenocarcinoma; PAAD, pancreatic adenocarcinoma; PCGC, pheochromocytoma and paraganglioma; PFS, progression-free survival; PPS, post-progression survival; PRAD, prostate adenocarcinoma; RCC, renal cell carcinoma; READ, rectum adenocarcinoma; RFS, relapse-free survival; SARC, sarcoma; SKCM, skin cutaneous melanoma; STAD, stomach adenocarcinoma; TCGA, The Cancer Genome Atlas; TGCT, testicular germ cell tumors; THCA, thyroid carcinoma; THYM, thymoma; TIDE, tumor immune dysfunction

and exclusion; TIMER2, Tumor Immune Estimation Resource, version 2; TMB, tumor mutational burden; TPM, transcripts per million; TMPO, thymopoietin; Treg, regulatory T cell; UCEC, uterine corpus endometrial carcinoma; UCS, uterine carcinosarcoma

## Declarations

### Conflict of Interest

The authors declare that the research was conducted in the absence of any commercial or financial relationships that could be construed as a potential conflict of interest.

### Author Contributions

JHZ, YXC, and ZYL participated in the conception and design of the study. JHZ, YKC, and JYW contributed to data acquisition, statistical analysis and technical support. YYL, JHC LZC and ZQJ contributed to literature search and revised the manuscript for important intellectual content. HTT, DTZ, and QPY interpreted the data produced and edited the drafts of the manuscript. All authors contributed to the article and approved the submitted version.

### Funding

This work was supported by the Special Fund Project of Guangdong Science and Technology (210728156901524, 210728156901519), Medical Scientific Research Foundation of Guangdong Province, China (grant number A2021432, B2021448), Shantou Medical Science and Technology Planning Project (grant number 210521236491457, 210625106490696, 220518116490772, 220518116490933). Administration of Traditional Chinese Medicine of Guangdong Province project 202205092315428030

### Acknowledgments

We thank Kan Wang for administrative assistance and Editage ([www.editage.cn](http://www.editage.cn)) for English language editing.

## References

1. Blum A, Wang P, Zenklusen JC (2018) SnapShot: T CGA-Analyzed Tumors. *Cell* 173(2):530. doi:10.1016/j.cell.2018.03.059
2. Tomczak K, Czerwińska P, Wiznerowicz M (2015) The Cancer Genome Atlas (TCGA): an immeasurable source of knowledge. *Contemp Oncol (Pozn)* 19(1A):A68–A77. doi:10.5114/wo.2014.47136
3. Clough E, Barrett T (2016) The Gene Expression Omnibus Database. *Methods Mol Biol* 1418:93–110. doi:10.1007/978-1-4939-3578-9\_5

4. Li C, Zhang Y, Yang Q, Ye F, Sun SY, Chen ES et al (2016) Nusap modulates the dynamics of kinetochore microtubules by attenuating microtubule depolymerisation activity. *Rep* 6(1):18773
5. Ribbeck K, Groen AC, Santarella R, Bohnsack M, Raemaekers T, Köcheret T et al (2006) NuSAP, a mitotic RanGTP target that stabilizes and cross-links microtubules. *Mol Biol Cell* 17(6):2646–2660. doi:10.1091/mbc.e05-12-1178
6. Kokkinakis DM, Liu X, Neuner RD (2005) Modulation of cell cycle and gene expression in pancreatic tumor cell lines by methionine deprivation (methionine stress): implications to the therapy of pancreatic adenocarcinoma. *Mol Cancer Ther* 4(9):1338–1348. doi:10.1158/1535-7163.MCT-05-0141
7. Ryu B, Kim DS, Deluca AM, Alani RM (2007) Comprehensive expression profiling of tumor cell lines identifies molecular signatures of melanoma progression. *PLoS ONE* 2(7):e594. doi:10.1371/journal.pone.0000594
8. Gordon CA, Gong X, Ganesh D, Brooks JD (2017) NUSAP1 promotes invasion and metastasis of prostate cancer. *Oncotarget* 8(18):29935–29950. doi:10.18632/oncotarget.15604
9. Dung-Tsa, Chen, Aejaz, Nasir, Aedin C et al (2010) Proliferative genes dominate malignancy-risk gene signature in histologically-normal breast tissue. *Breast Cancer Res Treat* 119(2):335–346. doi:10.1007/s10549-009-0344-y
10. Liu R, Guo CX, Zhou HH (2015) Network-based approach to identify prognostic biomarkers for estrogen receptor-positive breast cancer treatment with tamoxifen. *Cancer Biol Ther* 16(2):317–324. doi:10.1080/15384047.2014.1002360
11. Cuzick J, Swanson GP, Fisher G, Brothman AR, Berney DM, Reid JE et al (2011) Prognostic value of an rna expression signature derived from cell cycle proliferation genes in patients with prostate cancer: a retrospective study. *Lancet Oncol* 12(3):245–255. doi:10.1016/S1470-2045(10)70295-3
12. Li H, Zhang W, Yan M, Qiu J, Chen J, Sun X et al (2019) Nucleolar and spindle associated protein 1 promotes metastasis of cervical carcinoma cells by activating wnt/ $\beta$ -catenin signaling. *J Exp Clin Cancer Res* 38(1):33. doi:10.1186/s13046-019-1037-y
13. Roy S, Hooiveld GJ, Seehawer M, Caruso S, Heinzmann F, Schneider AT et al (2018) microRNA 193a-5p Regulates Levels of Nucleolar- and Spindle-Associated Protein 1 to Suppress Hepatocarcinogenesis. *Gastroenterology* 155(6):1951–1966e26. doi:10.1053/j.gastro.2018.08.032
14. Tang Z, Kang B, Li C, Chen T, Zhang Z (2019) GEPIA2: an enhanced web server for large-scale expression profiling and interactive analysis. *Nucleic Acids Res* 47(W1):W556–W560. doi:10.1093/nar/gkz430
15. Chen F, Chandrashekar DS, Varambally S, Creighton CJ (2019) Pan-cancer molecular subtypes revealed by mass-spectrometry-based proteomic characterization of more than 500 human cancers. *Nat Commun* 10(1):5679. doi:10.1038/s41467-019-13528-0
16. Bardou P, Mariette J, Escudié F, Djemiel C, Klopp C (2014) jvenn: an interactive Venn diagram viewer. *BMC Bioinformatics* 15(1):293. doi:10.1186/1471-2105-15-293

17. Fridman W, Galon J, Dieunosjean M, Cremer I, Fisson S, Damotte D (2011) Immune infiltration in human cancer: prognostic significance and disease control. *Curr Top Microbiol Immunol* 344:1–24. doi:10.1007/82\_2010\_46
18. Steven A, Seliger B (2108) The Role of Immune Escape and Immune Cell Infiltration in Breast Cancer. *Breast Care (Basel)* 13(1):16–21. doi:10.1159/000486585
19. Chen X, Song E (2019) Turning foes to friends: targeting cancer-associated fibroblasts. *Nat Rev Drug Discov* 18(2):99–115. doi:10.1038/s41573-018-0004-1
20. Kwa MQ, Herum KM, Brakebusch C (2019) Cancer-associated fibroblasts: how do they contribute to metastasis? *Clin Exp Metastasis* 36(2):71–86. doi:10.1007/s10585-019-09959-0
21. Raemaekers T, Ribbeck K, Beaudouin J, Annaert W, Camp MV, Stockmans I et al (2003) NuSAP, a novel microtubule-associated protein involved in mitotic spindle organization. *J Cell Biol* 162(6):1017–1029. doi:10.1083/jcb.200302129
22. Ribbeck K, Raemaekers T, Carmeliet G, Mattaj IW (2007) A role for NuSAP in linking microtubules to mitotic chromosomes. *Curr Biol* 17(3):230–236. doi:10.1016/j.cub.2006.11.050
23. Bosch AV, Raemaekers T, Denayer S, Torrekens S, Smets N, Moermans K et al (2010) NuSAP is essential for chromatin-induced spindle formation during early embryogenesis. *J Cell Sci* 123(Pt 19):3244–3255. doi:10.1242/jcs.063875
24. Ping X, Li L, Xing G, Tian C, Yin Y, He F et al (2011) ATM-mediated NuSAP phosphorylation induces mitotic arrest. *Biochem Biophys Res Commun* 404(1):413–418. doi:10.1016/j.bbrc.2010.11.135
25. Chou HY, Wang TH, Lee SC, Hsu PH, Tsai MD, Chang CL et al (2011) Phosphorylation of NuSAP by Cdk1 regulates its interaction with microtubules in mitosis. *Cell Cycle* 10(23):4083–4089. doi:10.4161/cc.10.23.18200
26. Mills CA, Suzuki A, Arceci A, Mo JY, Duncan A, Salmon ED et al (2017) Nucleolar and spindle-associated protein 1 (NUSAP1) interacts with a SUMO E3 ligase complex during chromosome segregation. *J Biol Chem* 292(42):17178–17189. doi:10.1074/jbc.M117.796045
27. Chen L, Yang L, Qiao F, Hu X, Li S, Yao L et al (2015) High Levels of Nucleolar Spindle-Associated Protein and Reduced Levels of BRCA1 Expression Predict Poor Prognosis in Triple-Negative Breast Cancer. *PLoS One*. 10(10):e0140572. Published 2015 Oct 20. doi:10.1371/journal.pone.0140572
28. Nie J, Wang H, He F, Huang H (2010) Nusap1 is essential for neural crest cell migration in zebrafish. *Protein Cell* 1(3):259–266. doi:10.1007/s13238-010-0036-8
29. Zhang X, Pan Y, Fu H, Zhang J (2018) Nucleolar and Spindle Associated Protein 1 (NUSAP1) Inhibits Cell Proliferation and Enhances Susceptibility to Epirubicin In Invasive Breast Cancer Cells by Regulating Cyclin D Kinase (CDK1) and DLGAP5 Expression. *Med Sci Monit* 24:8553–8564. doi:10.12659/MSM.910364
30. Roy S, Hooiveld GJ, Seehawer M, Caruso S, Heinzmann F, Schneider AT et al (2018) microRNA 193a-5p Regulates Levels of Nucleolar- and Spindle-Associated Protein 1 to Suppress Hepatocarcinogenesis. *Gastroenterology* 155(6):1951–1966e26. doi:10.1053/j.gastro.2018.08.032

31. Ling B, Wei P, Xiao J, Cen B, Huang W (2021) Nucleolar and spindle-associated protein 1 promotes non-small cell lung cancer progression and serves as an effector of myocyte enhancer factor 2D. *Oncol Rep* 45(3):1044–1058. doi:10.3892/or.2020.7918
32. hang Y, Huang K, Cai H, Chen S, Jiang P (2020) The role of nucleolar spindle-associated protein 1 in human ovarian cancer. *J Cell Biochem* 121(11):4397–4405. doi:10.1002/jcb.29661
33. Xu ZY, Wang Y, Xiong J, Cui FX, Peng H (2020) NUSAP1 knockdown inhibits cell growth and metastasis of non-small-cell lung cancer through regulating BTG2/PI3K/Akt signaling. *J Cell Physiol* 235(4):3886–3893. doi:10.1002/jcp.29282
34. Kretschmer C, Sterner-Kock A, Siedentopf F, Schoenegg W, Kemmner W et al (2011) Identification of early molecular markers for breast cancer. *Mol Cancer*. 10(1):15. Published 2011 Feb 11. doi:10.1186/1476-4598-10-15
35. Joyce JA, Fearon DT (2015) T cell exclusion, immune privilege, and the tumor microenvironment. *Science* 348(6230):74–80. doi:10.1126/science.aaa6204
36. Komohara Y, Fujiwara Y, Ohnishi K, Takeya M (2016) Tumor-associated macrophages: Potential therapeutic targets for anti-cancer therapy. *Adv Drug Deliv Rev* 99(Pt B):180–185. doi:10.1016/j.addr.2015.11.009

## Figures

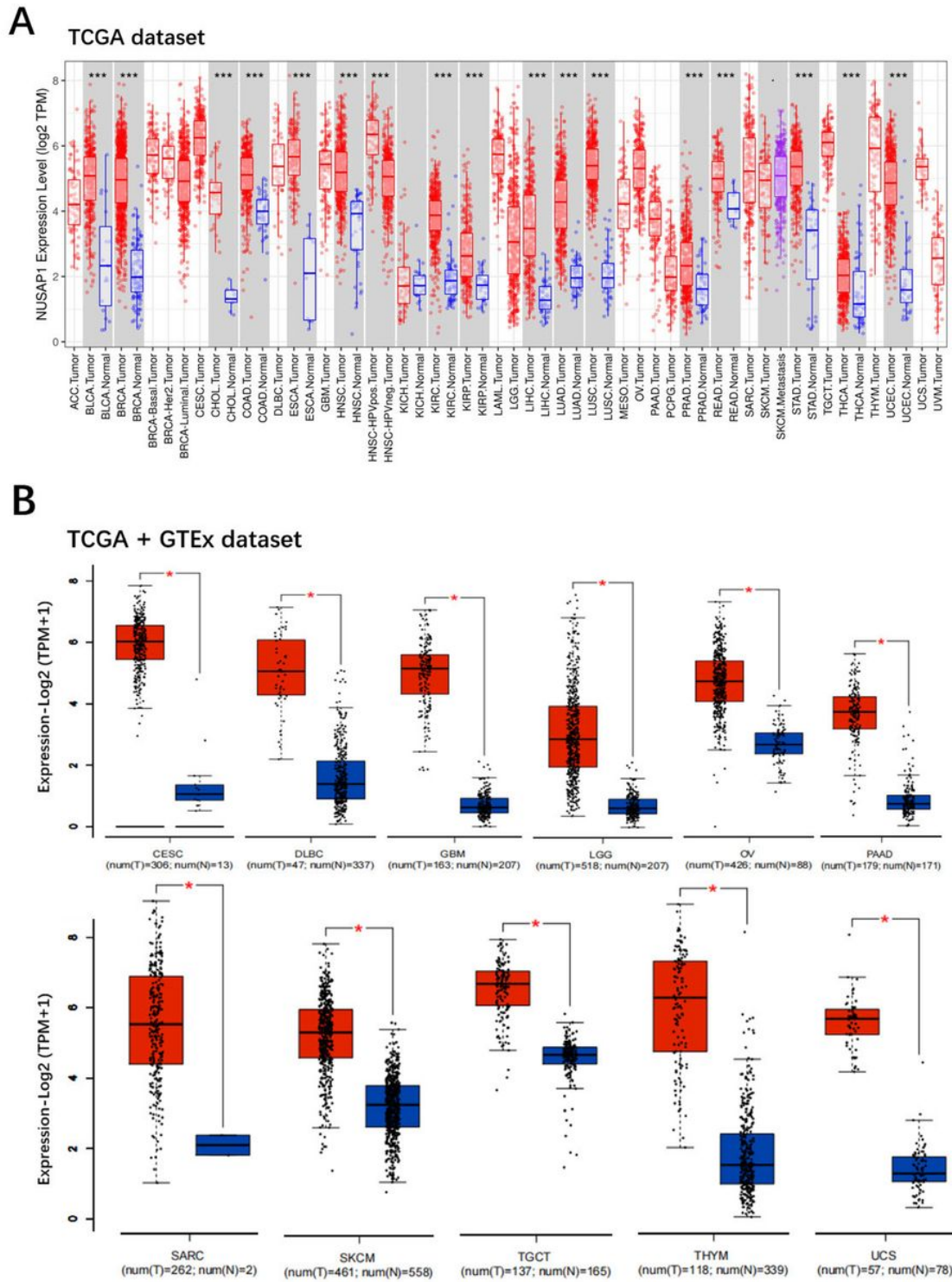


Figure 1

Legend not included with this version

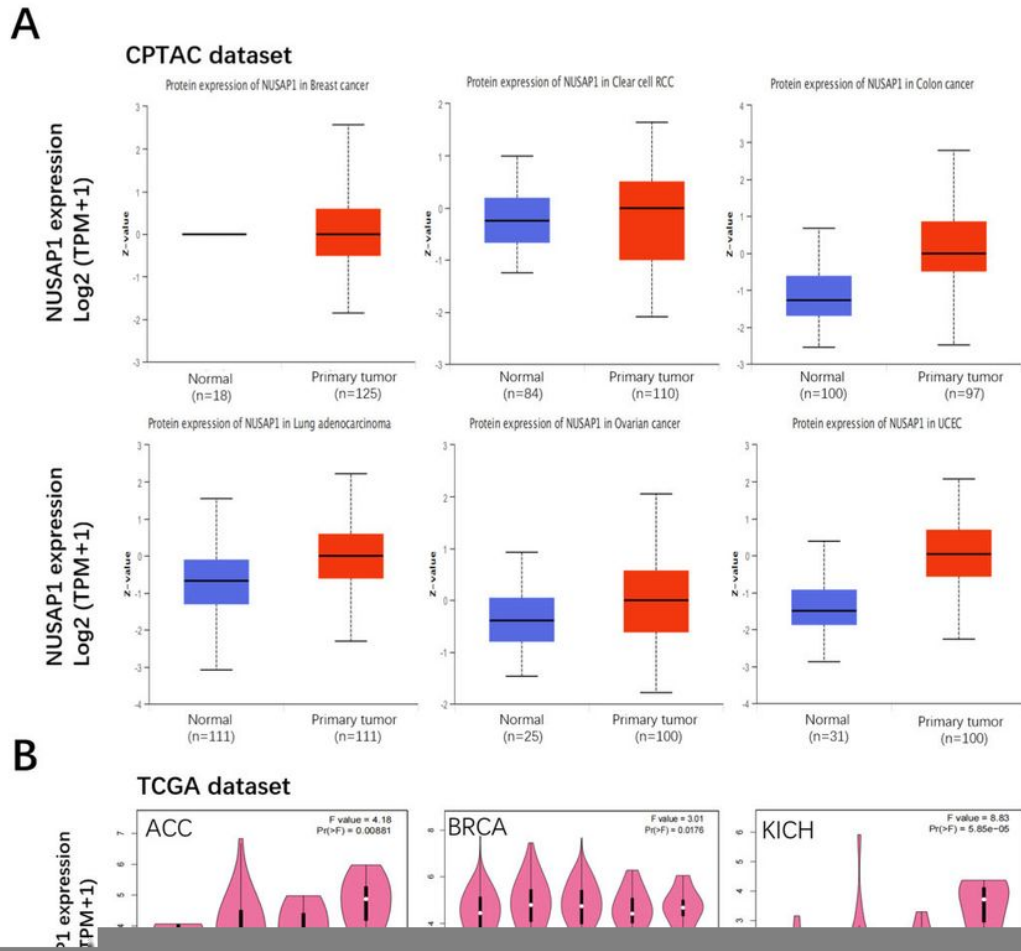
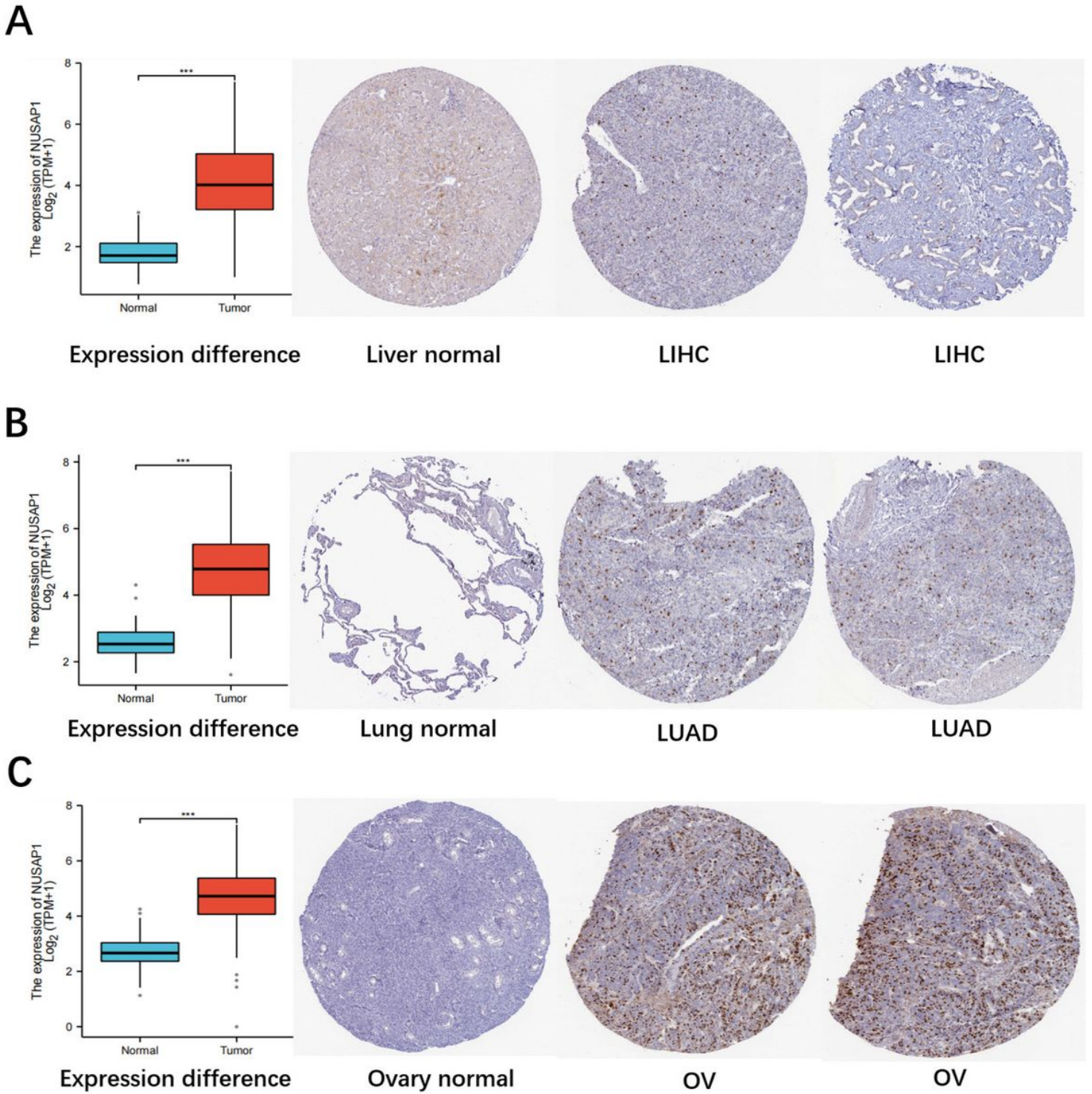


Figure 2

Legend not included with this version



**Figure 3**

Legend not included with this version

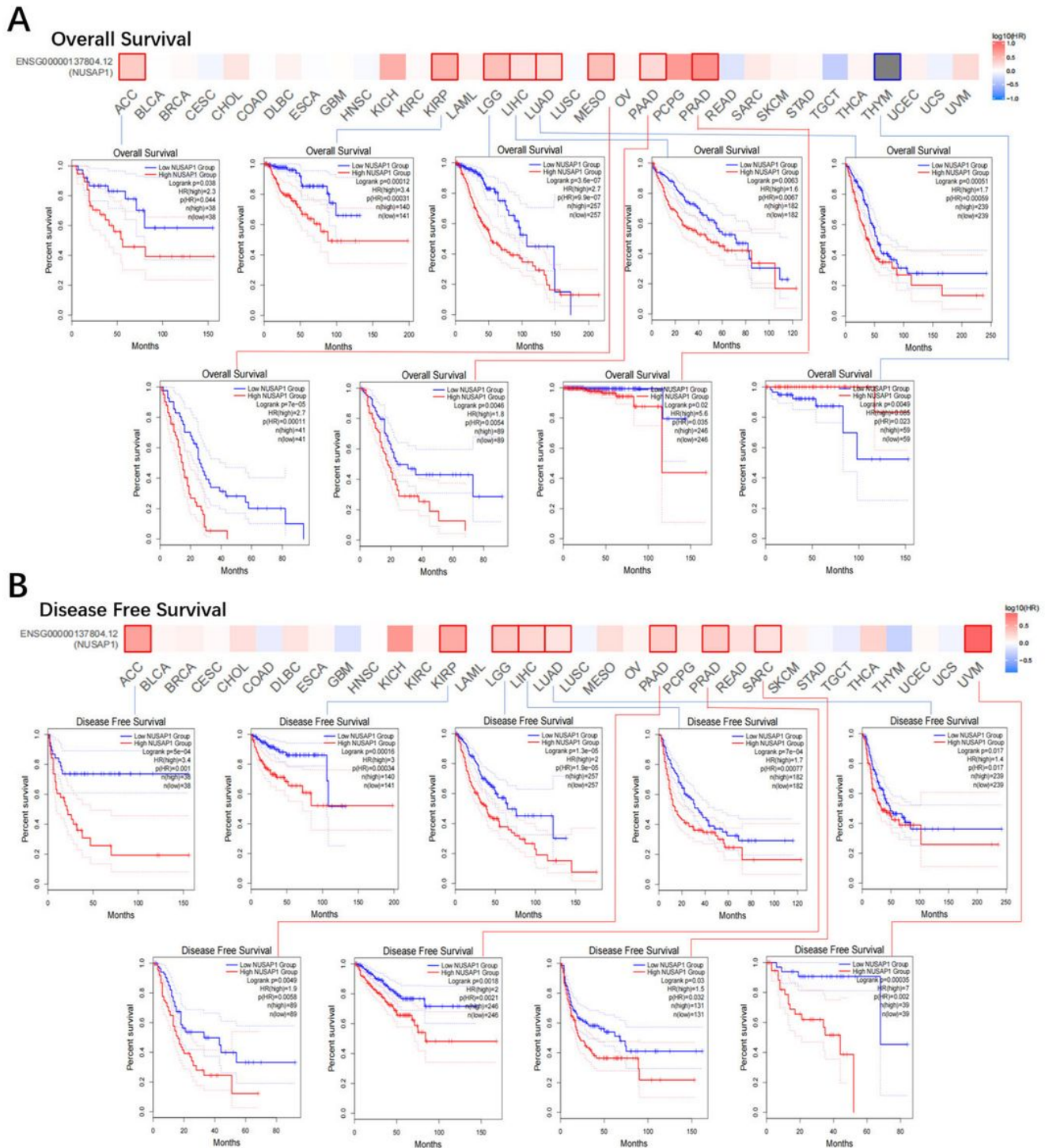
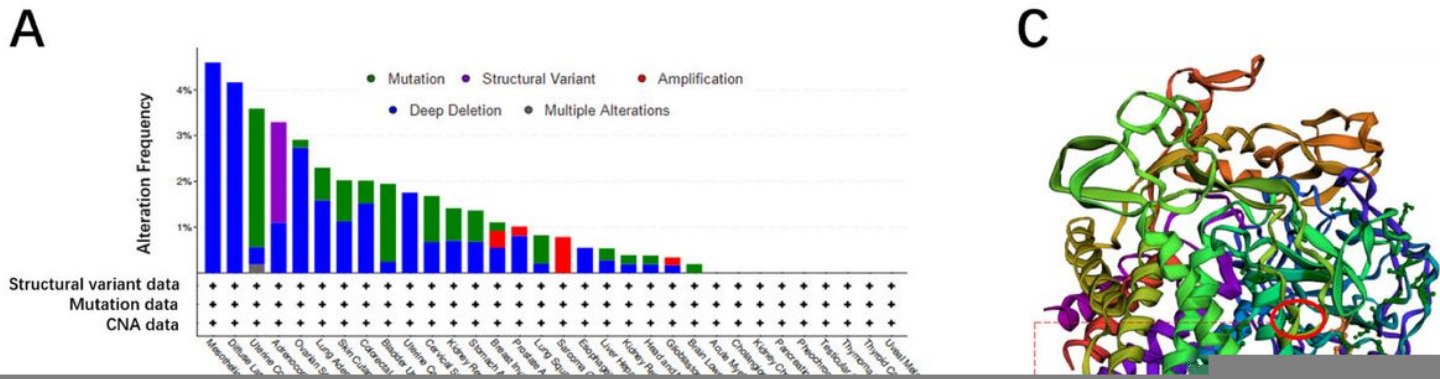


Figure 4

Legend not included with this version



**Figure 5**

Legend not included with this version

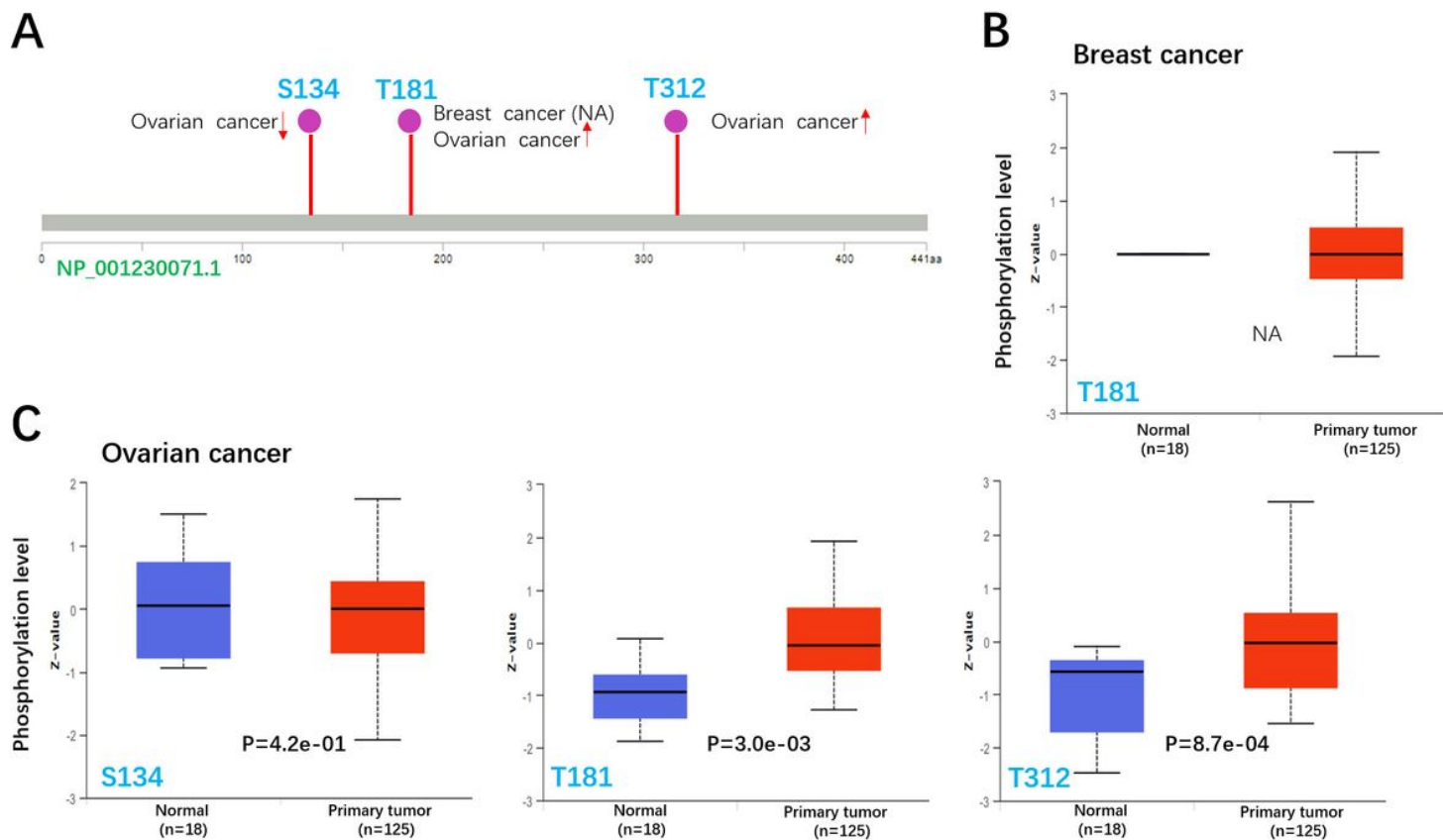


Figure 6

Legend not included with this version

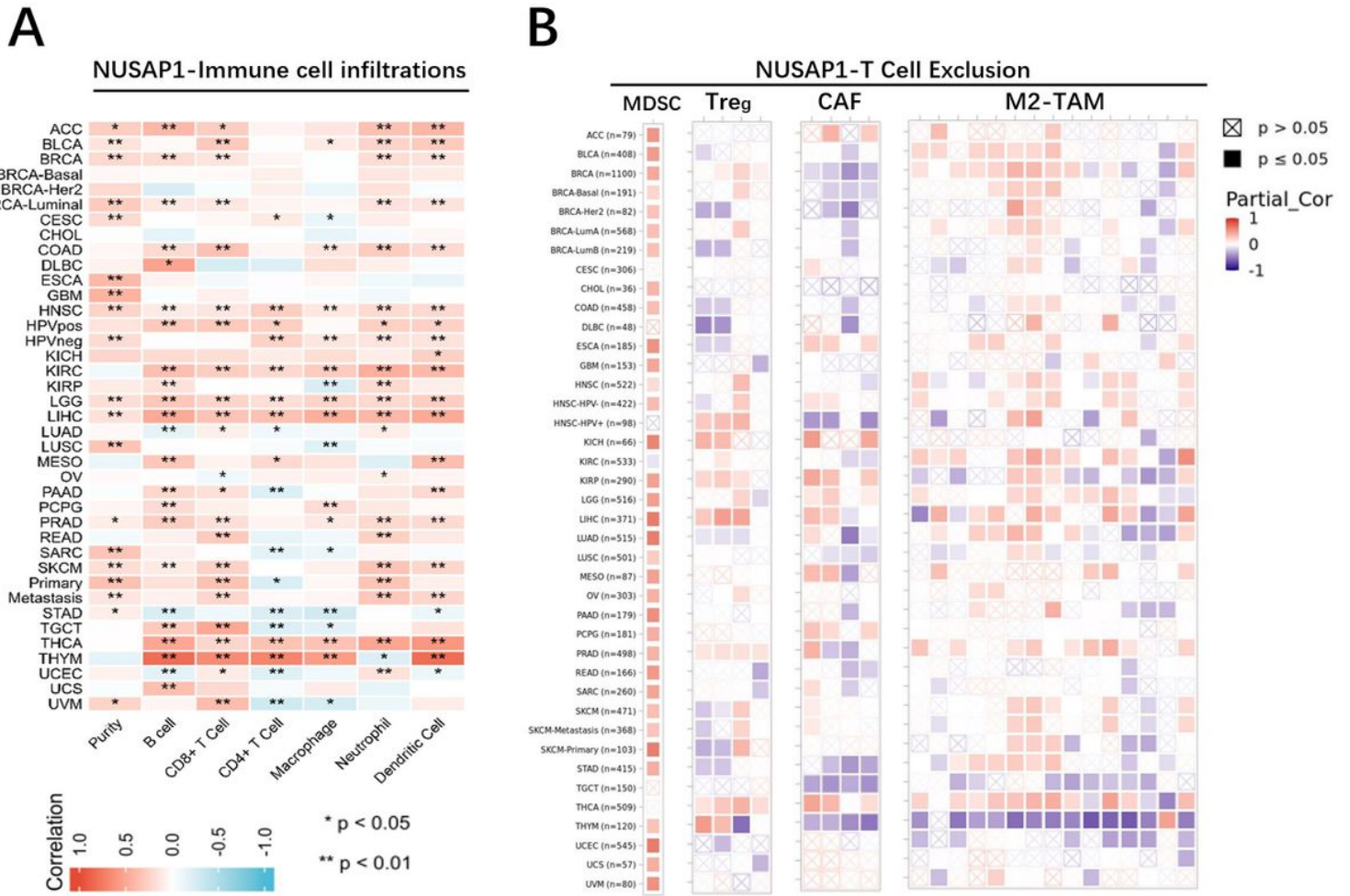
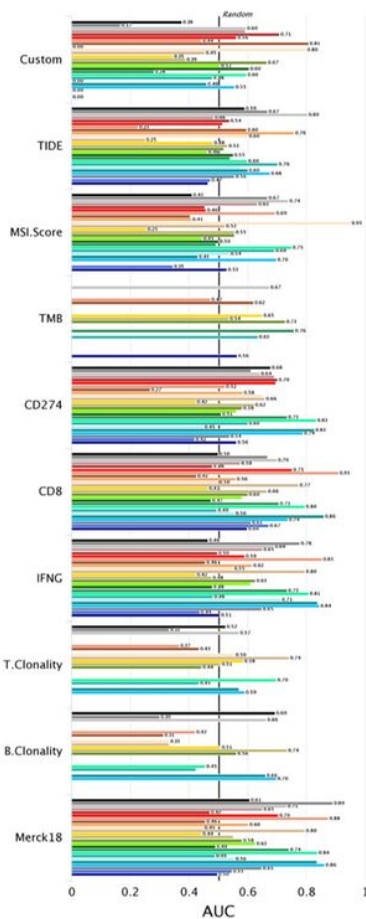


Figure 7

Legend not included with this version

**A**



- Zhao2019\_PD1\_Glioblastoma\_Pre  
Pos = 8, Neg = 7
- Zhao2019\_PD1\_Glioblastoma\_Post  
Pos = 6, Neg = 3
- VanAllen2015\_CTLA4\_Melanoma  
Pos = 19, Neg = 23
- Uppaluri2020\_PD1\_HNSC\_Pre  
Pos = 8, Neg = 15
- Uppaluri2020\_PD1\_HNSC\_Post  
Pos = 9, Neg = 13
- Ruppini2021\_PD1\_NSCLC  
Pos = 7, Neg = 15
- Riaz2017\_PD1\_Melanoma\_Ipi.Prog  
Pos = 4, Neg = 22
- Riaz2017\_PD1\_Melanoma\_Ipi.Naive  
Pos = 6, Neg = 19
- Prat2017\_PD1\_NSCLC-HNSC-Melanoma\_Nanostring  
Pos = 21, Neg = 12
- Nathanson2017\_CTLA4\_Melanoma\_Pre  
Pos = 4, Neg = 5
- Nathanson2017\_CTLA4\_Melanoma\_Post  
Pos = 4, Neg = 11
- Miao2018\_ICB\_Kidney\_Clear  
Pos = 20, Neg = 13
- McDermott2018\_PDL1\_Kidney\_Clear  
Pos = 20, Neg = 61
- Mariathasan2018\_PDL1\_Bladder\_mUC  
Pos = 68, Neg = 230
- Liu2019\_PD1\_Melanoma\_Ipi.Prog  
Pos = 16, Neg = 31
- Liu2019\_PD1\_Melanoma\_Ipi.Naive  
Pos = 33, Neg = 41
- Lauss2017\_ACT\_Melanoma  
Pos = 10, Neg = 15
- Kim2018\_PD1\_Gastric  
Pos = 12, Neg = 33
- Hugo2016\_PD1\_Melanoma  
Pos = 14, Neg = 12
- Hee2020\_PD1\_NSCLC\_Oncomine  
Pos = 9, Neg = 12
- Gide2019\_PD1\_Melanoma  
Pos = 19, Neg = 22
- Gide2019\_PD1+CTLA4\_Melanoma  
Pos = 21, Neg = 11
- Chen2016\_PD1\_Melanoma\_Nanostring\_Ipi.Prog  
Pos = 6, Neg = 9
- Chen2016\_CTLA4\_Melanoma\_Nanostring  
Pos = 5, Neg = 11
- Braun2020\_PD1\_Kidney\_Clear  
Pos = 201, Neg = 94

**B**

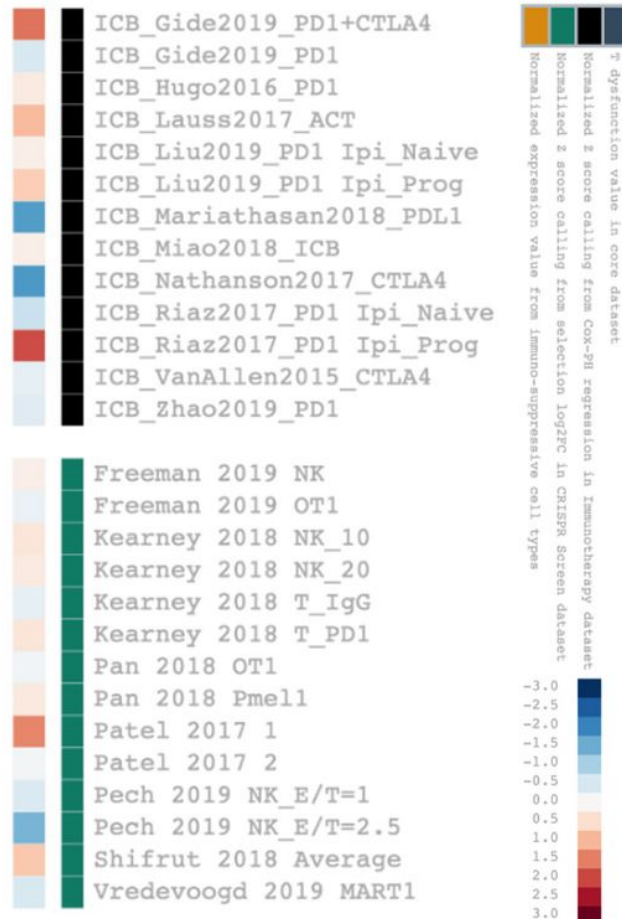


**Figure 8**

Legend not included with this version

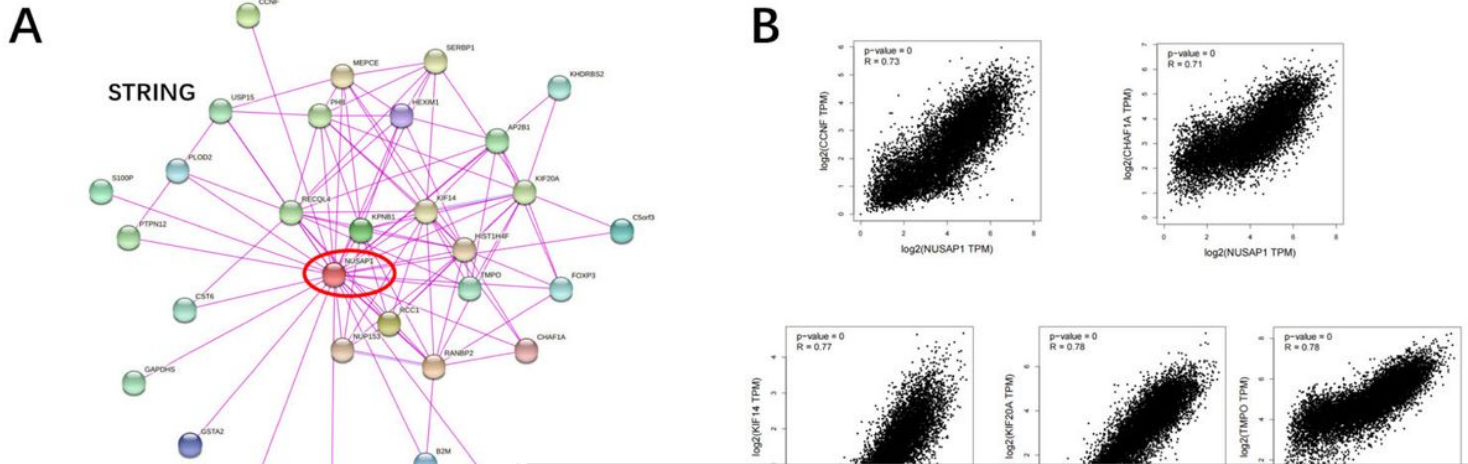


**Figure 9**

Legend not included with this version